SUPPLEMENTAL FIGURE 1: A) Hematoxylin and eosin staining of unwounded skin shows the epidermal and dermal morphology of *IL-22*$^{-/-}$ skin is similar to WT skin. Bars = 100 μm. Quantification of hair follicle number and hair cycle stage in WT and *IL-22*$^{-/-}$ skin at 7 weeks of age. n = 35-50 hair follicles in 6 mice. B) Quantification of hyperproliferative epidermal area in large (8mm) WT and *IL-22*$^{-/-}$ wounds. n = 6 wounds for each timepoint (2 wounds from 3 mice for each of 2 independent experiments). n.s. indicates not significant. C) Proliferation of epidermal cells of WT or *IL-22*$^{-/-}$ mice is similar 3 days post wounding with 2 mm punch biopsies as indicated by immunostaining of skin sections with antibodies against Ki67. D) Quantification of the number of Ki67+ cells per field of view in the leading edge of WT and *IL-22*$^{-/-}$ wounds. n = 6 wounds from 6 individual mice for each timepoint. E) Quantification of % reepithelialization in WT and *IL-22*$^{-/-}$ mice at indicated timepoints after wounding with indicated biopsy size. n = 18 mice (6 wounds from 6 mice for each of 3 independent experiments). Rate was determined using linear regression to calculate the slope of the re-epithelialization for WT and *IL-22*$^{-/-}$ wounds. Data are mean +/- SEM.

SUPPLEMENTAL FIGURE 2: A) Real time PCR analysis of *CD45* mRNA expression in WT or *IL-22*$^{-/-}$ wounds 3 days after wounding. n = 6 mice for each genotype. Skin sections of WT and *IL-22*$^{-/-}$ mice 3 days after wounding were immunostained with antibodies against CD45. B) Skin sections of WT and *IL-22*$^{-/-}$ mice 3 days after wounding were immunostained with isolectin GS-IB4 to mark blood vessels. C) Skin sections of WT and *IL-22*$^{-/-}$ mice 5 days after wounding were immunostained with antibodies against cathelicidin, an antimicrobial peptide induced during wounding. LE indicates leading edge of wound. Bars = 100μm.

SUPPLEMENTAL FIGURE 3: A) Representative FACS plots keratinocyte isolation. α6 integrin+ and GFP+ cells withing the live (propidium iodide negative) gate were purified by FACS to isolate keratinocytes from 7 week old *K14*-H2BGFP mice. B) Purity of isolated fibroblasts and keratinocytes was determined by real time PCR for mRNA expression of *vimentin* and *keratin 14* (*K14*) in isolated cells. C) Immunostaining with rabbit IgG and ER-TR7 shows specificity of staining for IL-22R.

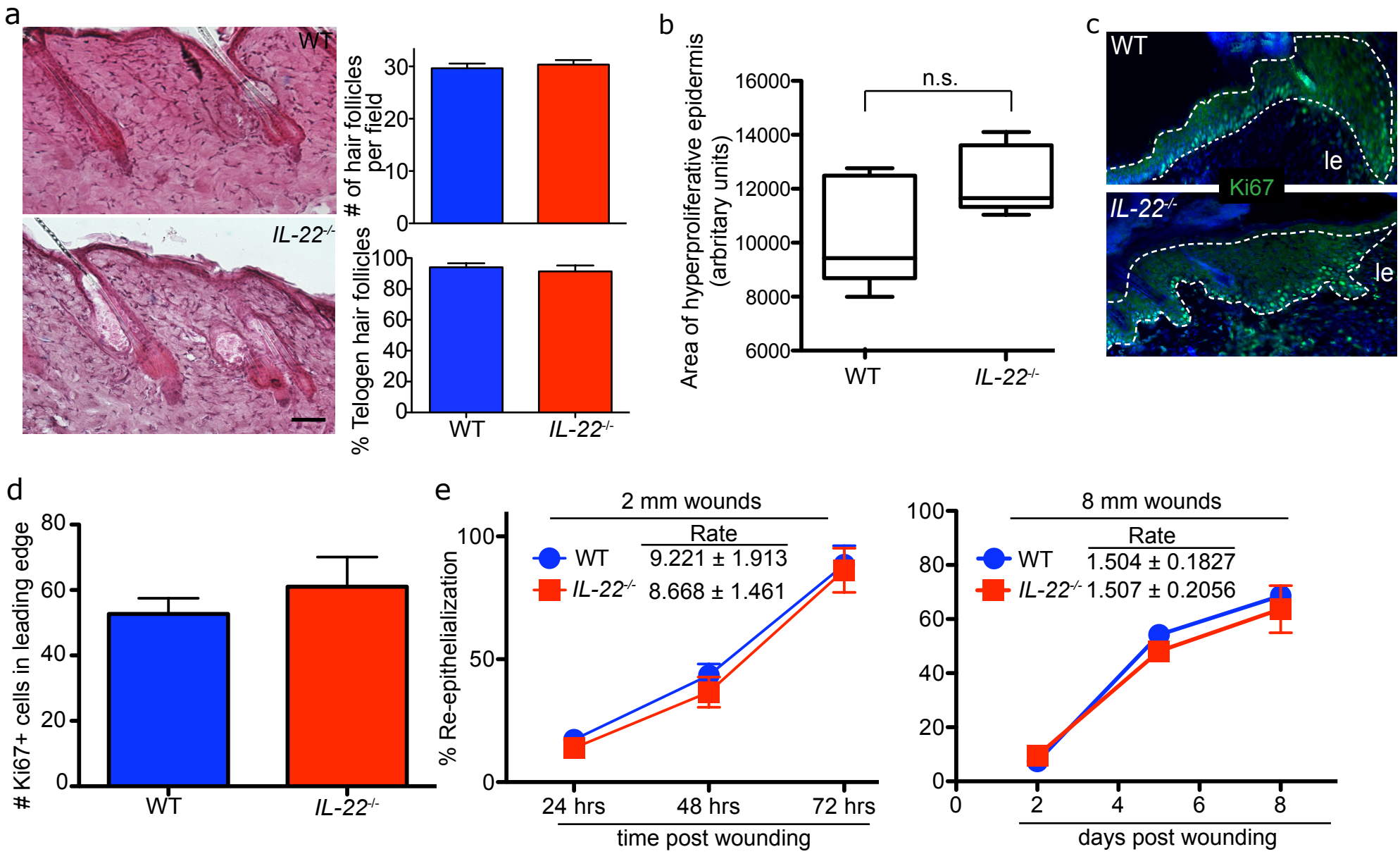
a
WT
IL-22-/-
# of hair follicles per field
% Telogen hair follicles
WT
IL-22-/-
b
Area of hyperproliferative epidermis (arbitrary units)
n.s.
WT
IL-22-/-
c
WT
le
Ki67
IL-22-/-
le
d
Ki67+ cells in leading edge
WT
IL-22-/-
e
2 mm wounds
Rate
WT 9.221 ± 1.913
IL-22-/- 8.668 ± 1.461
% Re-epithelialization
24 hrs
48 hrs
72 hrs
time post wounding
8 mm wounds
Rate
WT 1.504 ± 0.1827
IL-22-/- 1.507 ± 0.2056
days post wounding

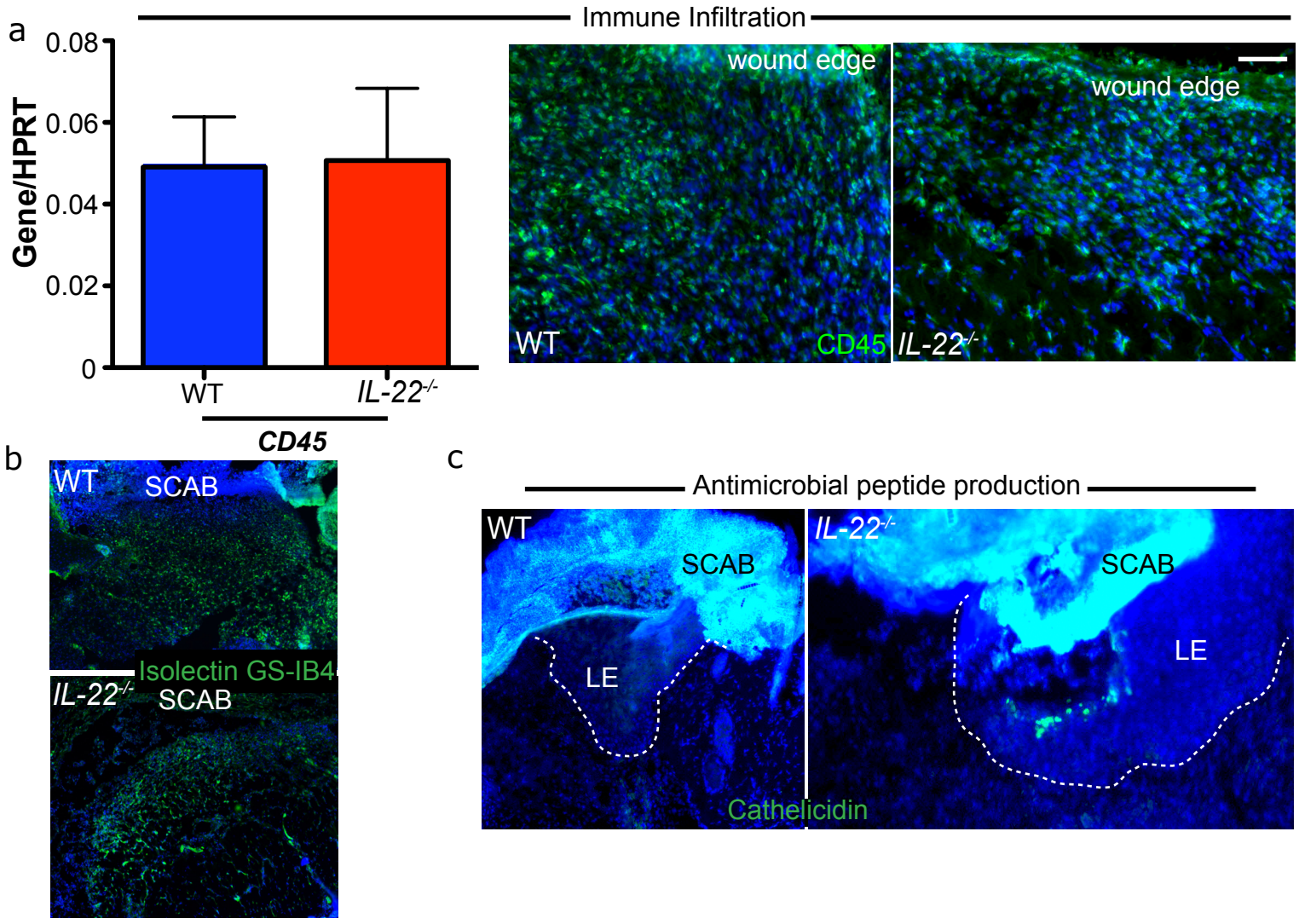
a
Immune Infiltration
Gene/HPRT
0.08
0.06
0.04
0.02
0
WT
IL-22-/-
CD45
wound edge
WT
CD45
wound edge
IL-22-/-
b
WT
SCAB
Isolectin GS-IB4
IL-22-/-
SCAB
c
Antimicrobial peptide production
WT
SCAB
LE
IL-22-/-
SCAB
LE
Cathelicidin

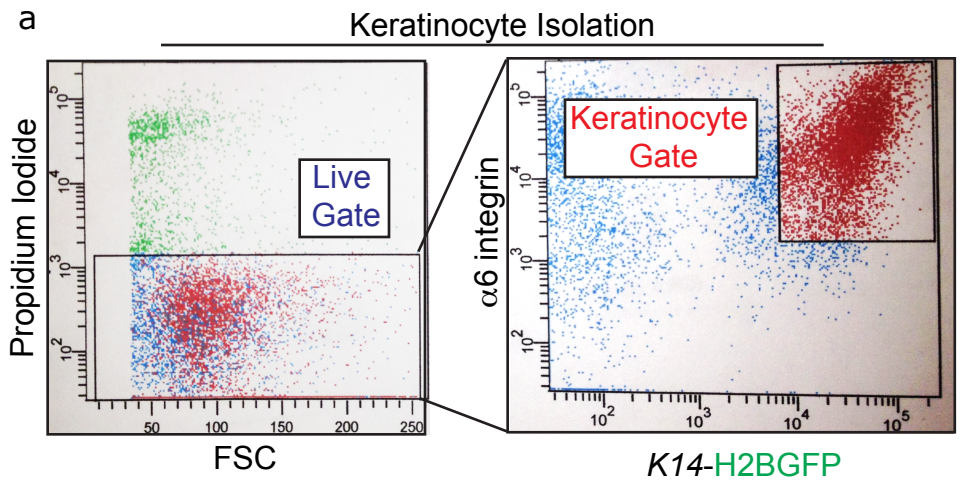
a
Keratinocyte Isolation
Propidium Iodide
Live Gate
FSC
α6 integrin
Keratinocyte Gate
K14-H2BGFP

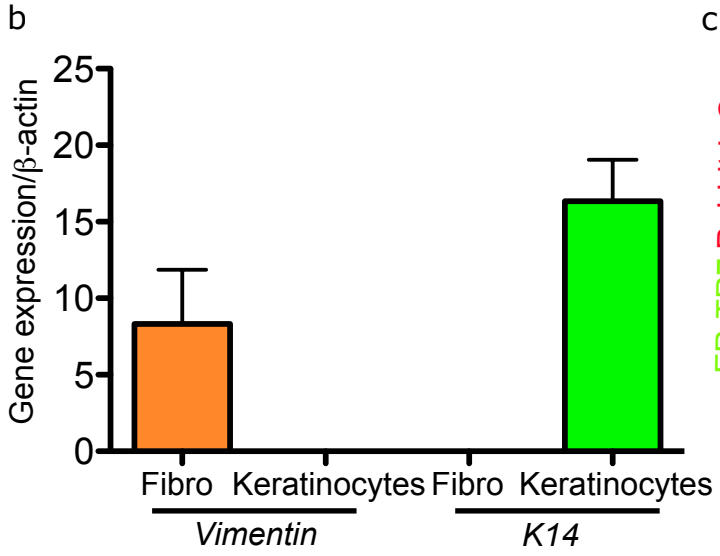
b
Gene expression/β-actin
25
20
15
10
5
0
Fibro
Keratinocytes
Fibro
Keratinocytes
Vimentin
K14

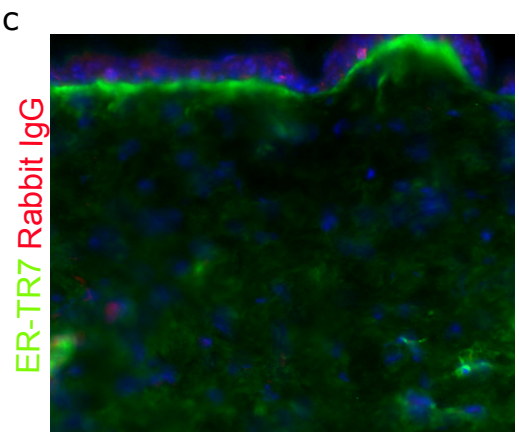
c
ER-TR7 Rabbit IgG